ACS chemical biology

Articles

pubs.acs.org/acschemicalbiology



# A FluoPol-ABPP PAD2 High-Throughput Screen Identifies the First Calcium Site Inhibitor Targeting the PADs

Daniel M. Lewallen,[†] Kevin L. Bicker,[†] Franck Madoux,[§] Peter Chase,[§] Lynne Anguish,[‡] Scott Coonrod,[‡] Peter Hodder,[§] and Paul R. Thompson*[,†,∥]

[†]Department of Chemistry, [‡]Lead ID, and [∥]The Kellogg School of Science and Technology, The Scripps Research Institute, Scripps Florida, 120 Scripps Way, Jupiter, Florida 33458, United States

[§]Baker Institute for Animal Health, College of Veterinary Medicine, Cornell University, Hungerford Hill Rd., Ithaca, New York 14850, United States

Supporting Information

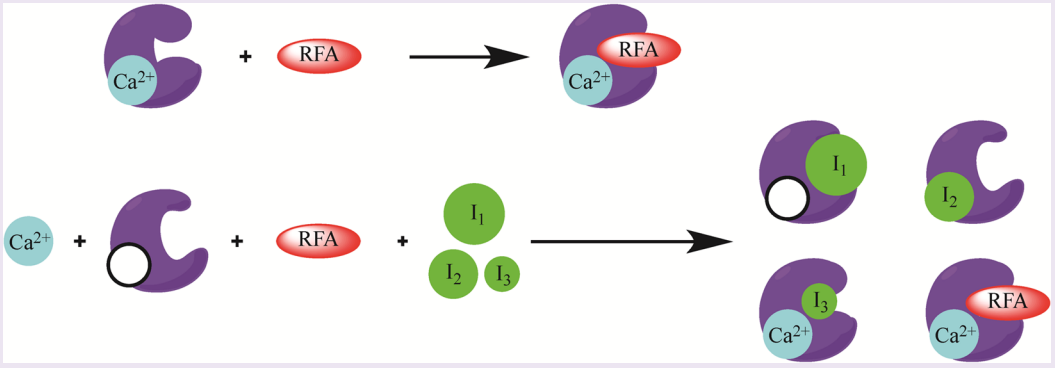


**ABSTRACT:** The protein arginine deiminases (PADs) catalyze the post-translational hydrolysis of peptidyl-arginine to form peptidyl-citrulline in a process termed deimination or citrullination. PADs likely play a role in the progression of a range of disease states because dysregulated PAD activity is observed in a host of inflammatory diseases and cancer. For example, recent studies have shown that PAD2 activates ER$\alpha$ target gene expression in breast cancer cells by citrullinating histone H3 at ER target promoters. To date, all known PAD inhibitors bind directly to the enzyme active site. PADs, however, also require calcium ions to drive a conformational change between the inactive apo-state and the fully active calcium bound holoenzyme, suggesting that it would be possible to identify inhibitors that bind the apoenzyme and prevent this conformational change. As such, we set out to develop a screen that can identify PAD2 inhibitors that bind to either the apo or calcium bound form of PAD2. Herein, we provide definitive proof of concept for this approach and report the first PAD inhibitor, ruthenium red ($K_i$ of 17 $\mu$M), to preferentially bind the apoenzyme.

The protein arginine deiminases (PADs) catalyze the post-translational hydrolysis of peptidyl-arginine to form peptidyl-citrulline in a process termed deimination or citrullination (Figure 1A).[1] These enzymes have garnered significant attention over the past several years because PAD activity is dysregulated in cancer and a host of inflammatory diseases (*e.g.*, rheumatoid arthritis, lupus, ulcerative colitis, Alzheimer's disease, and multiple sclerosis).[1,2] Although it is unclear how the PADs contribute to such a disparate number of diseases, common links include a role for PAD4 in promoting neutrophil extracellular trap (NET) formation and regulating gene transcription.[1,3] Further evidence that upregulated PAD activity plays a role in these various diseases comes from the demonstration that Cl-amidine, a potent pan-PAD inhibitor, or analogues show efficacy in animal models of cancer,[4] rheumatoid arthritis,[5] lupus,[6] thrombosis, spinal cord injury,[7] and ulcerative colitis.[8]

Although dysregulated PAD4 activity is typically associated with these diseases, more recent work suggests that PAD2 also plays an important role in both extracellular trap formation[9] and in gene regulation.[10,11] Thus, it is possible that PAD4 and PAD2 carry out similar/related functions during disease progression. Regarding gene regulation, PAD4 was previously implicated in regulating ER target gene expression via citrullination of histone H4Arg3 at ER target gene promoters. More recently, we carried out a detailed ChIP-chip study and found that PAD2 also plays a critical role in ER target gene activation *via* citrullination of histone H3Arg26 at ER target gene promoters.[11] Additionally, we found that PAD2 expression is highly correlated with HER2 expression across more than 60 breast cancer cell lines. Consistently, other

**Received:** November 12, 2013
**Accepted:** January 17, 2014
**Published:** January 27, 2014

   dx.doi.org/10.1021/cb400841k | *ACS Chem. Biol.* 2014, 9, 913–921

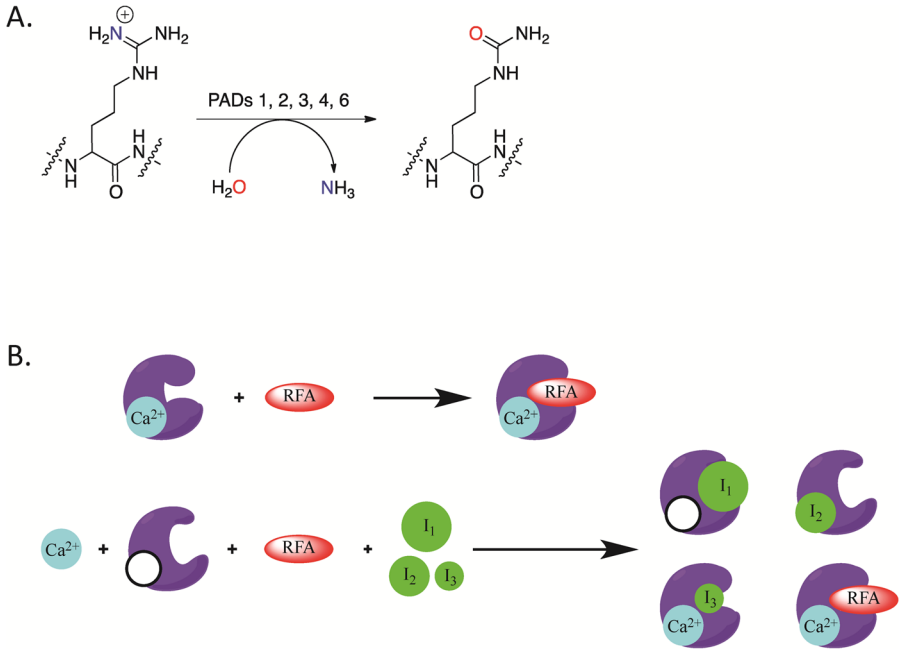


**Figure 1.** PAD reaction and PAD2 FluoPol-ABPP assay design. (A) PADs hydrolyze the positively charged guanidinium of peptidyl-arginine to form peptidyl-citrulline. (B) FluoPol-ABPP assay scheme to identify inhibitors for either the active or inactive conformation. At high calcium concentrations PAD2 exists only in the holo-form (top). At lower concentrations, PAD2 exists in the apo- or holo-form (bottom).

studies showed that PAD2 is one of 29 genes that represent a HER2 gene expression signature in primary tumors.[12] The importance of PAD2 in breast cancer is further confirmed by the finding that Cl-amidine inhibits the growth of MCF10DCIS xenografts, a mimic of ductal carcinoma *in situ* (DCIS), which express high levels of PAD2.[4] From a therapeutic standpoint, ~75% and 15% of all breast cancers are either ER or HER2+, respectively. Given that PAD2 likely plays an important role in the biology of both ER and HER2+ lesions, these observations suggest that PAD2 represents a therapeutic target for ~85−90% of all breast cancers in women.

Beyond breast cancer, PAD2-catalyzed histone citrullination has recently been implicated in the production of macrophage extracellular traps (METs) in adipose tissue from obese mice.[9] Given the emerging roles for extracellular traps in a range of disease states and the universal role of macrophages in promoting inflammation, further demonstration of the requirement for PAD2-mediated histone deimination in MET production suggests that PAD2 inhibitors may prove to be ideal therapeutics for a range of inflammatory diseases.

Given the therapeutic relevance of the PADs, significant effort has been made to develop PAD inhibitors.[13−19] While Cl-amidine reduces disease severity in the aforementioned animal models, it suffers from significant drawbacks, including a short *in vivo* half-life, poor bioavailability, and because Cl-amidine is an irreversible inhibitor, the potential for off-target effects.[13] To overcome these limitations and identify novel inhibitors, our lab previously developed plate- and gel-based screening assays that rely on rhodamine conjugated F-amidine (RFA), a PAD targeted activity based protein profiling (ABPP) reagent (Figure 1B).[20,21] In the plate-based assay, this probe, which consists of the core structure of F-amidine coupled (through a triazole) to rhodamine, is used to measure changes in PAD activity in the presence or absence of an inhibitor, using fluorescence polarization (FluoPol) as the readout. Using this assay, we identified streptonigrin as a PAD4-selective inhibitor.[20,21 22]

Although this RFA-based HTS assay shows great utility, it suffers from a number of limitations including a strong bias toward irreversible inhibitors and the fact that it preferentially identifies inhibitors targeting the fully active holoenzyme.[20] To identify inhibitors that bind to either the active or inactive calcium free conformations of PAD2, *i.e.*, apoPAD2, we modified this assay such that it is amenable to identifying these types of inhibitors (Figure 1C). Our strategy is based on the fact that the PADs are calcium-dependent enzymes that require high micromolar amounts of calcium (1−10 mM) for full activity; calcium activates the four known active PAD enzymes (*i.e.*, PADs 1−4) by >10,000-fold *in vitro*.[15,23] Inhibitors targeting the apoenzyme are particularly interesting because this enzyme form likely predominates inside the cell until a stimulating event.[24] Given these considerations, we hypothesized that by lowering the concentration of calcium it should be possible to identify inhibitors that bind the apoenzyme and thereby prevent the conformational changes that occur upon calcium-binding and enzyme activation. Since the active sites of apo and holoPAD4 show marked conformational differences between these two states, we expected this approach to identify unique chemotypes that preferentially bind to either form of the enzyme and therefore result in novel, potent, and selective inhibitors of the PAD family. Herein, we show for the first time that it is possible to identify small molecules that bind to the apoenzyme and report ruthenium red as a potent ($K_i$ of 17 $\mu$M) PAD2 inhibitor that is competitive with calcium and likely binds at the Calcium 3,4,5 site.

## RESULTS AND DISCUSSION

**Assay Design.** In our original FluoPol-ABPP HTS assay,[20] we used saturating (10 mM, 20× $K_{0.5}$) concentrations of calcium, such that >99% of the enzyme exists in the active,


dx.doi.org/10.1021/cb400841k | *ACS Chem. Biol.* 2014, 9, 913−921

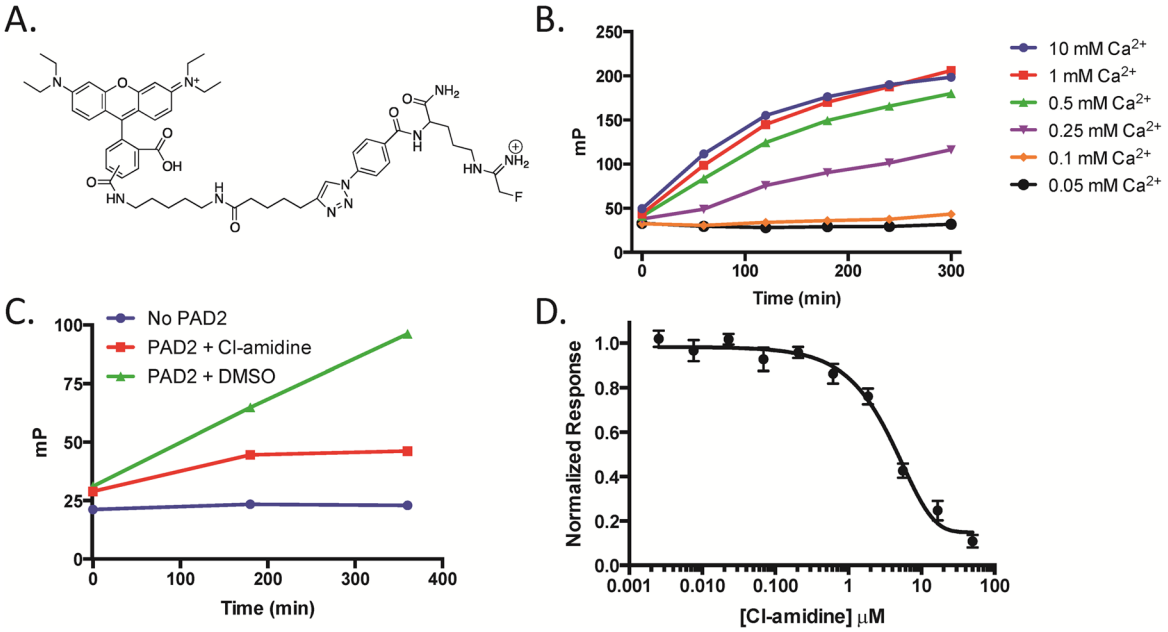


**Figure 2.** FluoPol-ABPP assay optimization. (A) Structure of rhodamine conjugated F-amidine (RFA). (B) Fluorescence polarization increases as a function of time and is dependent on the concentration of calcium. (C) Time course of the optimized conditions showing linearity out to 6 h and covalent inhibition by Cl-amidine. (D) $IC_{50}$ of Cl-amidine at 6 h.

calcium-bound, conformation. Since this concentration biases the assay toward compounds that bind the holoenzyme, we hypothesized that by lowering the calcium levels close to $K_{0.5}$, where the apo and holo states are present in roughly equivalent amounts, we would discover compounds that bind to either the apo- or holoenzyme. Since the apo state predominates under cellular conditions, compounds that bind the apoenzyme are particularly interesting because, like the DFG out protein kinase inhibitors,[25] we expect them to better prevent the conversion to the holo state (Figure 1).

Our assay is based on the reaction of PAD2 with RFA (Figures 1 and 2A), a PAD targeted activity based protein profiling (ABPP) reagent. When covalently bound to the PAD2 active site, slower rotation of the PAD2-RFA complex results in an observable increase in the emission of polarized light, *i.e.*, FluoPol.[26] By contrast, free RFA emits nonpolarized light as it rapidly rotates in solution. This assay has several advantages including a homogeneous readout and no washing, and RFA can be used to validate compounds in a gel-based screen to provide a semiquantitative read-out of inhibitor potency.

**Assay Optimization.** Our initial assay optimization started with our previously established PAD4 HTS conditions.[20] These conditions (PAD2 Screening buffer plus 10 mM $CaCl_2$) produce a robust FluoPol response with PAD2 (Figure 2B) that begins to level off at 3 h. Having demonstrated the feasibility of this FluoPol-ABPP assay for PAD2, we next evaluated the effect of lower calcium concentrations on the FluoPol response. The response is expected to decrease because the lower concentrations will shift the equilibrium from holoPAD2 toward apoPAD2. Indeed, as the calcium concentration is reduced, the rate of RFA labeling is slowed (Figure 2B). Given the robust FluoPol response at 350 $\mu$M $CaCl_2$ (~2× $K_{0.5}$), we used this concentration to further optimize the signal to baseline (S/B) and $Z'$ (a statistical measurement of assay dynamic range and data variation) and for the response to be linear over 6 h (Figure 2C). These conditions (see Methods) produced a robust S/B of ~4 and a $Z'$ factor ~0.7.

**Assay Reproducibility.** We next evaluated plate-to-plate and day-to-day variability by constructing a control plate containing DMSO (no PAD2) or Cl-amidine for the high controls, and DMSO (no inhibitors, low control) plus PAD2 to establish the sample field. The effect of DMSO on RFA labeling was further examined by pin-transferring 20 nL of DMSO from a source plate into a 384-well microtiter plate that already contained PAD2. Once transferred, the solution was preincubated for 20 min. During the actual screen this preincubation step facilitates diffusion throughout the well and also allows for any covalent or slow binding compounds to interact with the enzyme. RFA was then added, and after a 6 h incubation, FluoPol was measured and normalized against the controls. The 6 h time point was chosen to both maximize S/B and $Z'$ and minimize the number of robotic handling steps. A random well plot of four plates (1,488 wells) (Supplementary Figure S1) shows clear separation between the high (PAD2, DMSO) and both low controls (*i.e.*, no PAD2 and Cl-amidine). Because the Cl-amidine columns did not provide max inhibition, the no-PAD2 columns were used for all future $Z'$ calculations. Correlation plots (Supplementary Figure S1B) demonstrate that the assay shows excellent repeatability with the clustering of the controls and the DMSO sample field ($R^2$ = 0.86). $Z'$ factors are robust (~0.8 for each plate), and the S/B was near 4 (Supplementary Figure S1C), indicating that this assay is highly reproducible and shows very little deviation in the controls.

To further gauge the sensitivity and reproducibility of the assay, we determined the $IC_{50}$ for Cl-amidine, an irreversible pan-PAD inhibitor. For these studies, 7 replicates of 1/3 dilutions of Cl-amidine were pin transferred into the wells, and the FluoPol was measured after 6 h (Figure 2D). All replicates showed strong correlations, and we obtained good agreement in the $IC_{50}$ values obtained for Cl-amidine ($IC_{50(Cl\text{-}amidine)}$ = 4.4 ± 1 $\mu$M) at 6 h. Importantly, the $IC_{50}$ value is similar to the


dx.doi.org/10.1021/cb400841k | ACS Chem. Biol. 2014, 9, 913−921

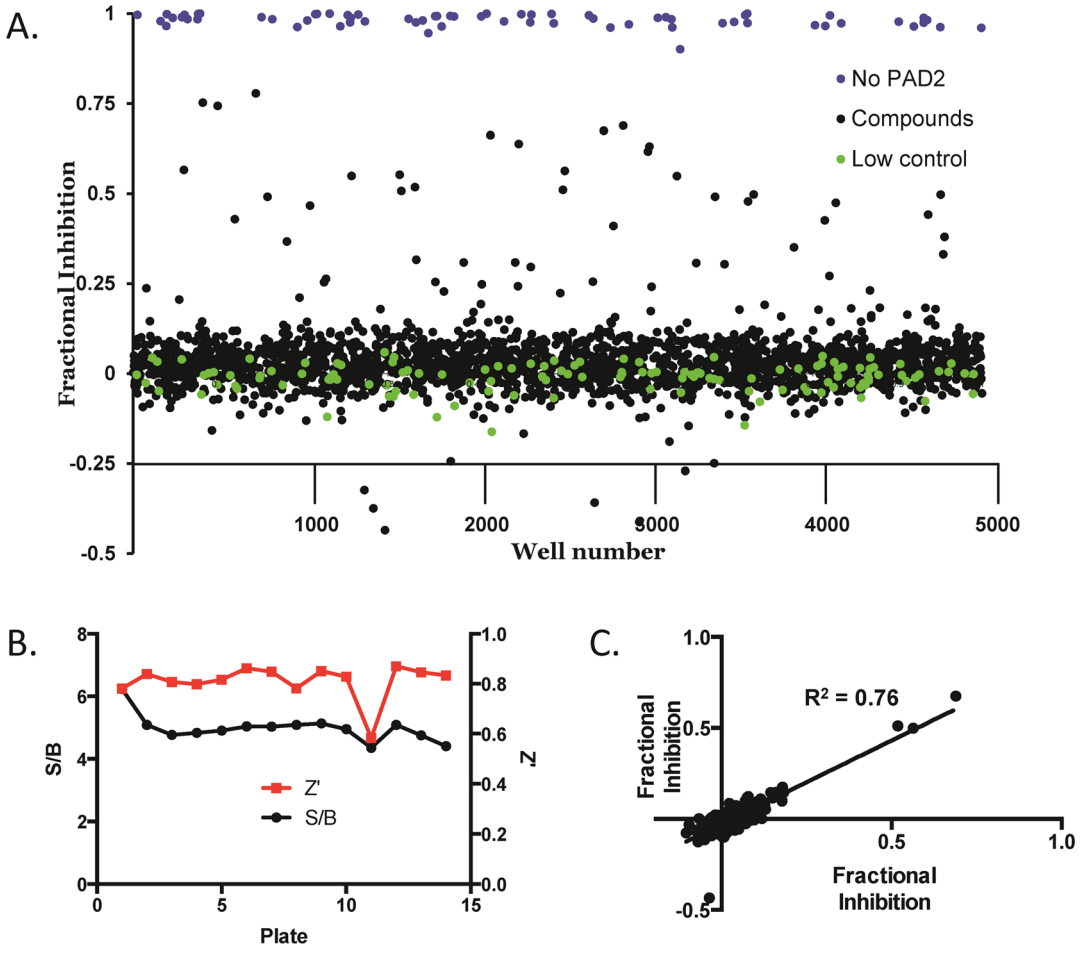


**Figure 3.** LOPAC screen. (A) Random well scatter of the 6 h normalized FluoPol values. (B) $Z'$ and S/B plots for each of the 12 plates. (C) Well correlation between 2 plate replicates.

value obtained *in vitro* using our standard PAD2 assay (17 ± 3.1 $\mu$M).[19]

**LOPAC Screen.** Using this optimized assay, we next screened the 1,280-compound LOPAC library (Sigma-Aldrich Library Of Pharmacologically Active Compounds) at 11 $\mu$M using the conditions and controls outlined above. A randomized-well activity scatter plot (Figure 3A) of the compounds (4,836 wells) shows strong separation between the controls (Figure 3B: average $Z'$ of 0.86 for the whole assay) and several potential inhibitors in-between. Using a typical assay cutoff,[27] the hit rate was calculated to be 0.8%. Comparing two replicates of the same LOPAC source plate (Figure 3C) shows the reproducibility of the assay for hit identification ($R^2$ = 0.76). The structures of a subset of the top hits are depicted in Figure 4A.

**Inhibitor Classification.** To classify inhibitors that bind apoPAD2, holoPAD2, or both, we developed a counterscreen that uses high calcium concentrations (10 mM); inhibitors that lose potency likely bind to apoPAD2 (due to the equilibrium shift), whereas no loss in potency implies that they bind either holoPAD2 or both forms of the enzyme. Incubating serial dilutions of the top LOPAC inhibitors with RFA and PAD2 with 10 mM calcium for 3 h or 350 $\mu$M calcium for 6 h led to substantially different compound response curves (CRC) for the different compounds. Using a minimum 3-fold increase in $IC_{50}$ as our cutoff, we classified NSC 95937 (**1**), sanguinarine (**3**), and U-83836 (**4**) as calcium-insensitive and ruthenium red (**2**) as calcium-sensitive inhibitors (Figure 4A,B; Supplementary Table S1).

**Secondary Screen and Inhibitor Validation.** To validate these classifications, we used our gel-based ABPP assay.[20] In this assay, PAD2 is incubated with compound, RFA, and either low (125 $\mu$M) or high (10 mM) calcium for 1 h or 30 min, respectively. On the basis of this analysis, compounds **1** and **3** show calcium-independent inhibition of PAD2, whereas **2** shows a strong decrease in percent inhibition at the higher concentration of calcium (Figure 4C,D; Supplementary Table S1). These trends were generally conserved when using less inhibitor (Supplementary Figure S2). The one exception is **4**, which showed no inhibition at low calcium but strong inhibition at high calcium when used at 100 $\mu$M. Notably, this pattern was reversed at lower inhibitor concentrations (Supplementary Figure S2), leading us to discard **4** as a possible artifact.

Compound **1** (NSC95397) contains a reactive quinone moiety and is known to irreversibly inhibit Cdc25,[28] whereas **2** (ruthenium red) is an inorganic complex that binds specifically to calcium-binding proteins such as calmodulin and has been shown to block calcium flux through calcium ion channels.[29,30] Compound **3** (sanguinarine) is a plant alkaloid isolated from the root of *Sanguinaria canadensis*[31] and has been demonstrated to target a variety of known cellular proteins including the phosphatases MKP-1[32] and PP2C.[33]


dx.doi.org/10.1021/cb400841k | *ACS Chem. Biol.* 2014, 9, 913–921

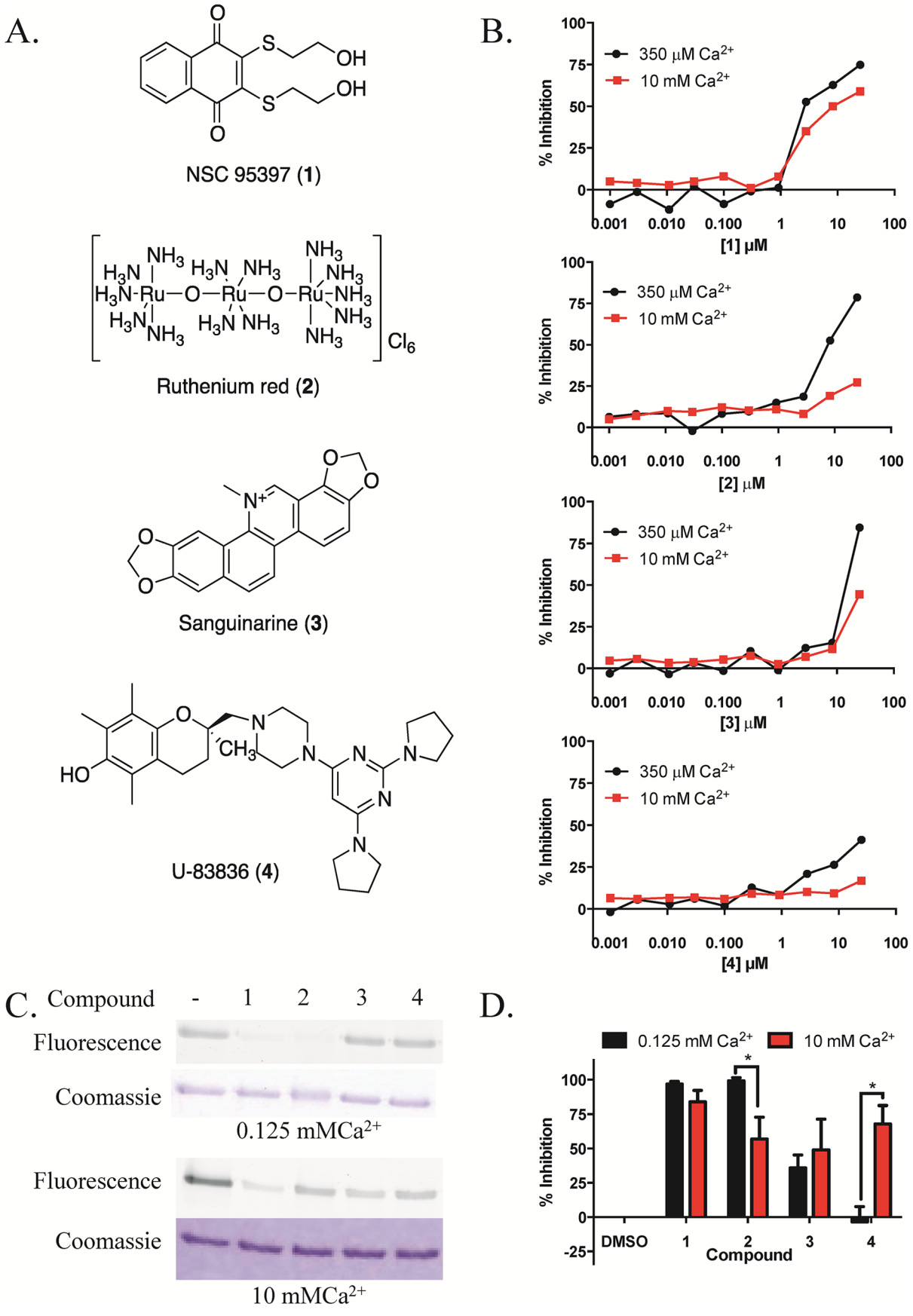


**Figure 4.** LOPAC hits and CRCs. (A) Structures of the four top hits identified from the LOPAC library. (B) CRC curves for the four LOPAC compounds with low (350 $\mu$M) and high (10 mM) calcium. (C) RFA gel-based counterscreen of PAD2 with 100 $\mu$M inhibitor and either low (0.125 mM) or high (10 mM) calcium. (D) Quantified fluorescence from panel C, *indicates $p < 0.05$.


dx.doi.org/10.1021/cb400841k | ACS Chem. Biol. 2014, 9, 913−921

**Inhibitor Kinetics.** After confirming that compounds **1**−**3** inhibit PAD2, we determined their potencies and mechanisms of inhibition. Initially, progress curves were generated for compounds **1**−**3** (Supplementary Figure S3). For compounds **2** and **3** product formation is linear with respect to time, consistent with their being reversible inhibitors. By contrast, the progress curves are nonlinear in the presence of **1**, suggesting that this compound is an irreversible inhibitor. Indeed, **1** contains a reactive quinone. Inhibition is unlikely to be due to peroxide formation because this compound still inhibits PAD2 in the absence of reducing agent (Supplementary Figure S4) and catalase did not alter the inactivation rate (not shown). Since the substrate BAEE protects against enzyme inactivation (Supplementary Figure S3A), we reasoned that **1** was an irreversible inhibitor. Kinetic analyses confirmed that this was the case and that **1** modifies the PAD2 active site with a $k_{inact}/K_I$ of 1600 ± 300 $M^{-1}$ $min^{-1}$. Since this compound is only 5-fold more potent toward PAD3 and 2-fold more potent toward PAD4 when compared to PAD2, it is a pan-PAD inhibitor (Table 1).

**Table 1. Potency and Selectivity of 1, 2, and 3**

| PAD | NSC95397 (**1**) $k_{inact}/[K_I]$ ($M^{-1}$ $min^{-1}$) | ruthenium red (**2**) $K_i$ ($\mu$M) | sanguinarine (**3**) $K_i$ ($\mu$M) |
|---|---|---|---|
| PAD1 | 175 ± 10[c] | 30 ± 10[a] | 2000 ± 400[a] |
| PAD2 | 1600 ± 300 | 17 ± 6[b] | 100 ± 30[b] |
| PAD3 | 9150 ± 1400[c] | 25 ± 5[a] | 60 ± 5[a] |
| PAD4 | 4530 ± 240[c] | 10 ± 1[a] | 80 ± 10[a] |

[a]$K_i$ determined by Dixon analysis. [b]$K_i$ determined by Lineweaver−Burk analysis. [c]Approximated using $k_{obs}/[I]$.

Since **2** and **3** (Supplementary Figures S3B,C) are calcium-sensitive and -insensitive reversible inhibitors, we next determined their potency with respect to both the substrate BAEE and calcium. On the basis of visual inspection of the Lineweaver−Burk plots and the accuracy of fits, compound **3** appears to be competitive with the substrate BAEE, with a $K_i$ of 100 ± 30 $\mu$M, and noncompetitive with respect to calcium ($K_i$ = 500 ± 65 $\mu$M) (Supplementary Figure S5C and D, respectively; Supplementary Tables S2 and 3). Compound **3** also inhibits PADs 3 and 4 with similar potency ($K_i$ = 60 ± 5 $\mu$M for PAD3 and 80 ± 10 $\mu$M for PAD4) but is a relatively weak PAD1 inhibitor ($K_i$ = 2000 ± 400 $\mu$M; Table 1).

Unlike **3**, compound **2** potency is sensitive to the concentration of calcium. On the basis of visual inspection of the Lineweaver−Burk plots and the accuracies of the fits (reduced $\chi^2$), **2** is competitive with calcium ($K_i$ = 17 ± 6 $\mu$M) but noncompetitive with respect to the substrate BAEE ($K_i$ = 1050 ± 200 $\mu$M) (Supplementary Tables S2 and 3, Supplementary Figure S5A and B, respectively). That **2** is competitive with calcium confirms the previous observation that inhibitor efficacy is decreased in the presence of higher calcium concentrations and thus confirms our hypothesis that this HTS assay can identify calcium competitive inhibitors. Compound **2** is also most potent for PAD2 and also shows similar potency for the other PAD isozymes with apparent $K_i$ values of 30 ± 10 $\mu$M for PAD1, 25 ± 5 $\mu$M for PAD3, and 10 ± 1 $\mu$M for PAD4 based on Dixon plot analysis (Table 1). To rule out the possibility that **2** is leaching $Ru^{3+}$ and, as a consequence, the metal ion inhibits calcium binding and PAD2 activation by occupying the calcium binding sites in place of calcium, we generated progress curves in the presence of a similar amount of $RuCl_3$ and showed that $Ru^{3+}$ does not inhibit PAD2 activity (Supplementary Figure S3D).

**Inhibiting Cellular PAD Activity.** PAD2 is expressed in macrophages, and increased PAD activity is observed in response to stimuli such as LPS or TNF.[9,34] Specifically, previous studies have shown that LPS stimulates PAD2 activity in macrophages *via* calcium influx through L-type calcium channels.[34,35] Additionally, recent studies have suggested a role for PAD2 in regulating gene transcription *via* histone H3 deimination.[11] Therefore, we determined whether compounds **1**−**3** inhibit histone H3 citrullination in LPS stimulated RAW mouse macrophages. Using our previously established citrulline-specific probe Rh-PG,[36] we first confirmed that LPS stimulation increases H3 deimination (Figure 5A). All three

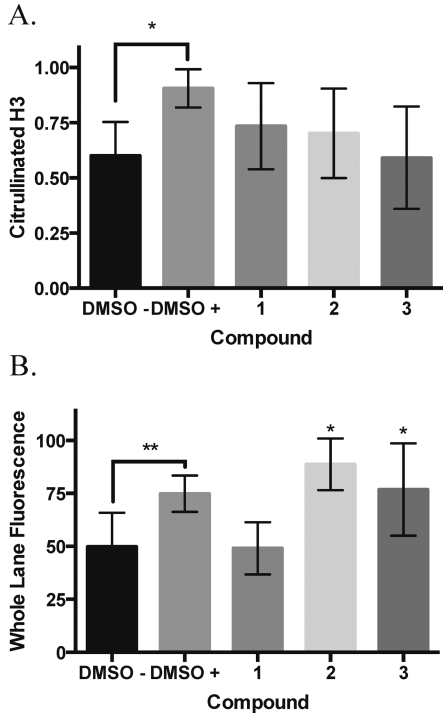


**Figure 5.** Efficacy of PAD2 inhibitors in cellular efficacy assays. (A) Citrullinated H3 levels were measured after treating RAW264.7 cells with LPS or DMSO control plus or minus compounds **1**, **2**, and **3** at 5 $\mu$M. (B) Stable PAD2 overexpressing HEK293T cells were stimulated with calcium ionophore in the presence or absence of compounds **1** (5 $\mu$M), **2** (5 $\mu$M), and **3** (1 $\mu$M). Cell extracts were treated with Rh-PG and proteins separated by SDS-PAGE, and the whole lane fluorescence was measured. Error bars show the standard deviation ($n$ = 4 for the panel A and $n$ = 6 for panel B). *$p$ value <0.05; **$p$ value <0.01.

inhibitors were able to prevent the increase in citrullination induced by LPS. However, it should be noted that the efficacy of **2** may be due to inactiviating the L-type calcium ion channels and therefore preventing calcium flux.[30−33]

To further determine if the cellular efficacy was due to direct inhibition of PAD2, or by some other pathway, we constructed a stable HEK 293T PAD2 overexpressing cell line (Supplementary Figure S6). Upon stimulation with Ca/ionophore in Locke's solution, we observed a robust increase in total protein citrullination using our citrulline-specific Rh-PG probe (Figure 5B). Unlike the previous RAW cell assay, only **1** showed efficacy in this model, indicating that the inhibition afforded by **2** and/or **3** may be due effects on calcium flux. While


dx.doi.org/10.1021/cb400841k | ACS Chem. Biol. 2014, 9, 913−921

encouraging, these results demonstrate the need to screen larger libraries to find more drug-like molecules that preferentially bind the apo form of the enzyme.

**Conclusions.** In conclusion, we have developed and optimized a FluoPol-ABPP based HTS for PAD2. We successfully identified compound **2** as a calcium competitive inhibitor that binds apoPAD2. Additionally, using this screening approach we identified a covalent inhibitor (**1**), as well as an active site competitive inhibitor (**3**). After full characterization, we show that **1** inhibits deimination in both cellular efficacy models. In total, these results demonstrate that our low calcium screen is a viable approach to discover novel PAD inhibitors.

## METHODS

**PAD2 HTS Assay Validation.** PAD2 Screening Buffer (8 μL of 50 mM HEPES pH 7.6, 150 mM NaCl, 1 mM TCEP, 350 μM $CaCl_2$, 0.01% pluronic acid) (column 1) and PAD2 (8 μL; 2 μM final) in Screening Buffer (columns 2−23) were added to a black 384-well microtiter plate (Greiner 784076) using a Beckman Coulter Flying Reagent Dispenser (FRD). Controls (column 1: DMSO (no PAD2, high control); column 2: 5 mM Cl-amidine (high control); and column 23: DMSO (no inhibitors, low control)) and source DMSO (100%) (columns 3−22) were pinned 2× using the 10 nL head on a Beckman Coulter BioMek NXP to achieve a final DMSO concentration of 0.4% v/v. After a 20 min incubation, RFA (2 μL; 75 nM final) in Screening Buffer was added using the FRD. The plates were read after incubating for 6 h at 37 °C using a PerkinElmer EnVision plate reader (Ex: 531, Em: 595).

**LOPAC Screen.** PAD2 Screening Buffer (8 μL; column 1) and PAD2 (8 μL; 2 μM final) in Screening Buffer (columns 2−23) were added to a black 384-well microtiter plate (Greiner 784076) using the FRD. Controls (column 1: DMSO (no PAD2, high control); column 2: 5 mM Cl-amidine (high control); and column 23: DMSO (no inhibitors, low control)) and LOPAC molecules (columns 3−22) were pinned 2× using the 10 nL head on a Beckman Coulter BioMek NXP to achieve a final concentration of 11 μM. After a 20 min incubation, RFA in Screening Buffer (2 μL; 75 nM final) was added using the FRD. The plates were read after incubating for 6 h at 37 °C as described above.

**Compound Response Curves (CRC).** PAD2 Screening Buffer (8 μL; column 1) and PAD2 (8 μL; 2 μM final) in Screening Buffer (columns 2−23) were added to a black 384-well microtiter plate (Greiner 784076) with the FRD. Controls (column 1: DMSO (no PAD2, high control); column 2: 5 mM Cl-amidine (high control); and column 23: DMSO (no inhibitors, low control)) and CRC molecules (columns 3−22) were pinned using the 100 nL head on a Beckman Coulter BioMek NXP to achieve a final concentration of 1 nM to 25 μM. After a 20 min incubation, RFA in Screening Buffer (75 nM final) was added using the FRD. The plates were read after incubating for 6 h at 37 °C as described above. $IC_{50}$ values were calculated by fitting the normalized inhibition data to eq 1:

$$\text{fractional activity} = 1/(1 + [\text{I}]/\text{IC}_{50}) \quad (1)$$

using Grafit 5.0.1.1 where [I] is the concentration of inhibitor.

**PAD2 High Calcium Counter Screen.** PAD2 High Calcium Screening Buffer (8 μL; 50 mM HEPES pH 7.6, 150 mM NaCl, 1 mM TCEP, 10 mM $CaCl_2$, 0.01% pluronic acid) (column 1) and PAD2 (8 μL; 2 μM final) in PAD2 High Calcium Screening Buffer (columns 2−23) were added to a black 384-well microtiter plate (Greiner 784076) using the FRD. Controls (column 1: DMSO (no PAD2, high control); column 2: 5 mM Cl-amidine (high control); and column 23: DMSO (no inhibitors, low control)) and CRC molecules (columns 3−22) were transferred with the 100 nL head on a Beckman Coulter BioMek NXP to achieve a final concentration of 1 nM to 25 μM. RFA in Screening Buffer (75 nM final) was added using the FRD. The plates were read after incubating for 6 h at 37 °C using a PerkinElmer EnVision plate reader as described above.

**Gel-Based Secondary Screens.** Gel-based secondary screens were performed analogously to a previously described method.[21] Briefly, PAD2 (1 μM final) was preincubated with inhibitor (10 or 100 μM final) in PAD2 Gel Screening Buffer (50 mM HEPES pH 7.6, 150 mM NaCl, 1 mM TCEP, 125 μM or 10 mM $CaCl_2$, 0.01% pluronic acid) for 20 min. RFA (5 μM final) was then added, and the reaction was incubated at 37 °C. The reaction was quenched after 1 h (125 μM $CaCl_2$) or 30 min (10 mM $CaCl_2$) with 6× SDS-PAGE loading buffer. The proteins were then separated on a 12% SDS-PAGE gel and imaged to 50 μm on a Typhoon 9410 (GE Healthcare) set at 580 nm. The fluorescent intensities were quantified using Image Quant. Percent inhibition was calculated by normalizing the fluorescence relative to the DMSO control ($n$ = 4).

***In Cellulo* PAD Inhibition.** RAW 264.7 cells (ATCC) were seeded in a 6-well tissue culture dish in DMEM. The next day, DMSO (10 μL) or compound (10 μL, 5 μM final) was added and incubated for 2 h. LPS (10 μL, 1 μg/mL final) or EtOH (10 μL) was added and incubated for 2 h. The cells were scraped, centrifuged (700$g$), and washed 2× with cold PBS. The pellet was resuspended in 800 μL of cold Lysis Buffer (50 mM PBS pH 7.4, 0.5% Triton, 2 mM PMSF, 0.02% $NaN_3$) and incubated 10 min. The nuclei were pelleted at 2,000$g$ for 10 min at 4 °C, washed with 400 μL of Lysis Buffer, then resuspended in 150 μL of cold 0.2 M HCl, and incubated overnight at 4 °C. The samples were centrifuged at 2,000$g$ to obtain the histone-containing supernatant. The proteins were labeled with Rh-PG, and their fluorescence was quantified as described previously.[36] The four replicates were evaluated for significance using a two-tailed $t$ test comparing the inhibitor-treated cells to DMSO-treated cells.

## ASSOCIATED CONTENT

### Supporting Information

Supplemental figures and tables as well as full methods. This material is available free of charge *via* the Internet at http://pubs.acs.org.

## AUTHOR INFORMATION

### Corresponding Author

*E-mail: Pthompso@scripps.edu.

### Notes

The authors declare no competing financial interest.

## ACKNOWLEDGMENTS

We thank P. Baillargeon and L. DeLuca (Lead Identification, Scripps Florida) for LOPAC screen compound management. This work is supported in part by TSRI and NIH grants GM079357 (PRT), DOD Era of Hope Scholar Award (W871XWH-07-1-0372) to S.C. and MH084512 to F.M., P.C., and P.H.

## REFERENCES

(1) Jones, J. E., Causey, C. P., Knuckley, B., Slack-Noyes, J. L., and Thompson, P. R. (2009) Protein arginine deiminase 4 (PAD4): Current understanding and future therapeutic potential. *Curr. Opin. Drug Discovery Dev. 12*, 616−627.

(2) Bicker, K. L., and Thompson, P. R. (2013) The protein arginine deiminases: Structure, function, inhibition, and disease. *Biopolymers 99*, 155−163.

(3) Rohrbach, A. S., Slade, D. J., Thompson, P. R., and Mowen, K. A. (2012) Activation of PAD4 in NET formation. *Front. Immunol. 3*, 360.

(4) McElwee, J. L., Mohanan, S., Griffith, O. L., Breuer, H. C., Anguish, L. J., Cherrington, B. D., Palmer, A. M., Howe, L. R., Subramanian, V., Causey, C. P., Thompson, P. R., Gray, J. W., and Coonrod, S. A. (2012) Identification of PADI2 as a potential breast cancer biomarker and therapeutic target. *BMC Cancer 12*, 500.

(5) Willis, V. C., Gizinski, A. M., Banda, N. K., Causey, C. P., Knuckley, B., Cordova, K. N., Luo, Y., Levitt, B., Glogowska, M., Chandra, P., Kulik, L., Robinson, W. H., Arend, W. P., Thompson, P.

R., and Holers, V. M. (2011) N-α-Benzoyl-N5-(2-chloro-1-iminoethyl)-l-ornithine amide, a protein arginine deiminase inhibitor, reduces the severity of murine collagen-induced arthritis. *J. Immunol. 186*, 4396−4404.
(6) Leffler, J., Martin, M., Gullstrand, B., Tydén, H., Lood, C., Truedsson, L., Bengtsson, A. A., and Blom, A. M. (2012) Neutrophil extracellular traps that are not degraded in systemic lupus erythematosus activate complement exacerbating the disease. *J. Immunol. 188*, 3522−3531.
(7) Lange, S., Gögel, S., Leung, K.-Y., Vernay, B., Nicholas, A. P., Causey, C. P., Thompson, P. R., Greene, N. D. E., and Ferretti, P. (2011) Protein deiminases: New players in the developmentally regulated loss of neural regenerative ability. *Dev. Biol. 355*, 205−214.
(8) Chumanevich, A. A., Causey, C. P., Knuckley, B. A., Jones, J. E., Poudyal, D., Chumanevich, A. P., Davis, T., Matesic, L. E., Thompson, P. R., and Hofseth, L. J. (2011) Suppression of colitis in mice by Cl-amidine: a novel peptidylarginine deiminase inhibitor. *Am. J. Physiol. Gastrointest. Liver Physiol. 300*, G929−G938.
(9) Mohanan, S., Horibata, S., McElwee, J. L., Dannenberg, A. J., and Coonrod, S. A. (2013) Identification of macrophage extracellular trap-like structures in mammary gland adipose tissue: a preliminary study. *Front. Immunol. 4*, 67.
(10) Cherrington, B. D., Morency, E., Struble, A. M., Coonrod, S. A., and Wakshlag, J. J. (2010) Potential role for peptidylarginine deiminase 2 (PAD2) in citrullination of canine mammary epithelial cell histones. *PLoS One 5*, e11768.
(11) Zhang, X., Bolt, M., Guertin, M. J., Chen, W., Zhang, S., Cherrington, B. D., Slade, D. J., Dreyton, C. J., Subramanian, V., Bicker, K. L., Thompson, P. R., Mancini, M. A., Lis, J. T., and Coonrod, S. A. (2012) Peptidylarginine deiminase 2-catalyzed histone H3 arginine 26 citrullination facilitates estrogen receptor α target gene activation. *Proc. Natl. Acad. Sci. U.S.A. 109*, 13331−13336.
(12) Bertucci, F., Borie, N., Ginestier, C., Groulet, A., Charafe-Jauffret, E., Adelaide, J., Geneix, J., Bachelart, L., Finetti, P., Koki, A., Hermitte, F., Hassoun, J., Debono, S., Viens, P., Fert, V., Jacquemier, J., and Birnbaum, D. (2004) Identification and validation of an ERBB2 gene expression signature in breast cancers. *Oncogene 23*, 2564−2575.
(13) Bicker, K. L., Anguish, L., Chumanevich, A. A., Cameron, M. D., Cui, X., Witalison, E., Subramanian, V., Zhang, X., Chumanevich, A. P., Hofseth, L. J., Coonrod, S. A., and Thompson, P. R. (2012) D-Amino acid based protein arginine deiminase inhibitors: Synthesis, pharmacokinetics, and in cellulo efficacy. *ACS Med. Chem. Lett. 3*, 1081−1085.
(14) Causey, C. P., Jones, J. E., Slack, J. L., Kamei, D., Jones, L. E., Subramanian, V., Knuckley, B., Ebrahimi, P., Chumanevich, A. A., Luo, Y., Hashimoto, H., Sato, M., Hofseth, L. J., and Thompson, P. R. (2011) The development of N-α-(2-carboxyl)benzoyl-N5-(2-fluoro-1-iminoethyl)-l-ornithine amide (o-F-amidine) and N-α-(2-carboxyl)-benzoyl-N5-(2-chloro-1-iminoethyl)-l-ornithine amide (o-Cl-amidine) as second generation protein arginine deiminase (PAD) inhibitors. *J. Med. Chem. 54*, 6919−6935.
(15) Knuckley, B., Causey, C. P., Jones, J. E., Bhatia, M., Dreyton, C. J., Osborne, T. C., Takahara, H., and Thompson, P. R. (2010) Substrate specificity and kinetic studies of PADs 1, 3, and 4 identify potent and selective inhibitors of protein arginine deiminase 3. *Biochemistry 49*, 4852−4863.
(16) Luo, Y., Arita, K., Bhatia, M., Knuckley, B., Lee, Y.-H., Stallcup, M. R., Sato, M., and Thompson, P. R. (2006) Inhibitors and inactivators of protein arginine deiminase 4: Functional and structural characterization. *Biochemistry 45*, 11727−11736.
(17) Luo, Y., Knuckley, B., Bhatia, M., Pellechia, P. J., and Thompson, P. R. (2006) Activity-based protein profiling reagents for protein arginine deiminase 4 (PAD4): Synthesis and in vitro evaluation of a fluorescently labeled probe. *J. Am. Chem. Soc. 128*, 14468−14469.
(18) Wang, Y., Li, P., Wang, S., Hu, J., Chen, X. A., Wu, J., Fisher, M., Oshaben, K., Zhao, N., Gu, Y., Wang, D., Chen, G., and Wang, Y. (2012) Anticancer peptidylarginine deiminase (PAD) inhibitors regulate the autophagy flux and the mammalian target of rapamycin complex 1 activity. *J. Biol. Chem. 287*, 25941−25953.
(19) Jones, J. E., Slack, J. L., Fang, P., Zhang, X., Subramanian, V., Causey, C. P., Coonrod, S. A., Guo, M., and Thompson, P. R. (2011) Synthesis and screening of a haloacetamidine containing library to identify PAD4 selective inhibitors. *ACS Chem. Biol. 7*, 160−165.
(20) Knuckley, B., Jones, J. E., Bachovchin, D. A., Slack, J., Causey, C. P., Brown, S. J., Rosen, H., Cravatt, B. F., and Thompson, P. R. (2010) A FluoPol-ABPP HTS assay to identify PAD inhibitors. *Chem. Commun. 46*, 7175−7177.
(21) Knuckley, B., Luo, Y., and Thompson, P. R. (2008) Profiling protein arginine deiminase 4 (PAD4): A novel screen to identify PAD4 inhibitors. *Bioorg. Med. Chem. 16*, 739−745.
(22) Bolzán, A. D., and Bianchi, M. S. (2001) Genotoxicity of streptonigrin: a review. *Mutat. Res. 488*, 25−37.
(23) Kearney, P. L., Bhatia, M., Jones, N. G., Yuan, L., Glascock, M. C., Catchings, K. L., Yamada, M., and Thompson, P. R. (2005) Kinetic characterization of protein arginine deiminase 4: A transcriptional corepressor implicated in the onset and progression of rheumatoid arthritis. *Biochemistry 44*, 10570−10582.
(24) Vossenaar, E. R., Radstake, T. R. D., van der Heijden, A., van Mansum, M. A. M., Dieteren, C., de Rooij, D.-J., Barrera, P., Zendman, A. J. W., and van Venrooij, W. J. (2004) Expression and activity of citrullinating peptidylarginine deiminase enzymes in monocytes and macrophages. *Ann. Rheum. Dis. 63*, 373−381.
(25) Garuti, L., Roberti, M., and Bottegoni, G. (2010) Non-ATP competitive protein kinase inhibitors. *Curr. Med. Chem. 17*, 2804−2821.
(26) Bachovchin, D. A., Brown, S. J., Rosen, H., and Cravatt, B. F. (2009) Identification of selective inhibitors of uncharacterized enzymes by high-throughput screening with fluorescent activity-based probes. *Nat. Biotechnol. 27*, 387−394.
(27) Hodder, P., Cassaday, J., Peltier, R., Berry, K., Inglese, J., Feuston, B., Culberson, C., Bleicher, L., Cosford, N. D., Bayly, C., Suto, C., Varney, M., and Strulovici, B. (2003) Identification of metabotropic glutamate receptor antagonists using an automated high-throughput screening system. *Anal. Biochem. 313*, 246−254.
(28) Lazo, J. S., Nemoto, K., Pestell, K. E., Cooley, K., Southwick, E. C., Mitchell, D. A., Furey, W., Gussio, R., Zaharevitz, D. W., Joo, B., and Wipf, P. (2002) Identification of a potent and selective pharmacophore for Cdc25 dual specificity phosphatase inhibitors. *Mol. Pharmacol. 61*, 720−728.
(29) Charuk, J. H., Pirraglia, C. A., and Reithmeier, R. A. (1990) Interaction of ruthenium red with Ca2(+)-binding proteins. *Anal. Biochem. 188*, 123−131.
(30) Tapia, R., and Velasco, I. (1997) Ruthenium red as a tool to study calcium channels, neuronal death and the function of neural pathways. *Neurochem. Int. 30*, 137−147.
(31) Han, M. H., Kim, S. O., Kim, G. Y., Kwon, T. K., Choi, B. T., Lee, W. H., and Choi, Y. H. (2007) Induction of apoptosis by sanguinarine in C6 rat glioblastoma cells is associated with the modulation of the Bcl-2 family and activation of caspases through downregulation of extracellular signal-regulated kinase and Akt. *Anticancer Drugs 18*, 913−921.
(32) Aburai, N., Yoshida, M., Ohnishi, M., and Kimura, K. (2010) Sanguinarine as a potent and specific inhibitor of protein phosphatase 2C in vitro and induces apoptosis via phosphorylation of p38 in HL60 cells. *Biosci. Biotechnol. Biochem. 74*, 548−552.
(33) Vogt, A., Tamewitz, A., Skoko, J., Sikorski, R. P., Giuliano, K. A., and Lazo, J. S. (2005) The benzo[c]phenanthridine alkaloid, sanguinarine, is a selective, cell-active inhibitor of mitogen-activated protein kinase phosphatase-1. *J. Biol. Chem. 280*, 19078−19086.
(34) Lee, H. J., Joo, M., Abdolrasulnia, R., Young, D. G., Choi, I., Ware, L. B., Blackwell, T. S., and Christman, B. W. (2010) Peptidylarginine deiminase 2 suppresses inhibitory B kinase activity in lipopolysaccharide-stimulated RAW 264.7 macrophages. *J. Biol. Chem. 285*, 39655−39662.
(35) Kim, Y., Moon, J. S., Lee, K. S., Park, S. Y., Cheong, J., Kang, H. S., Lee, H. Y., and Kim, H. D. (2004) $Ca^{2+}$/calmodulin-dependent

protein phosphatase calcineurin mediates the expression of iNOS through IKK and NF-kappaB activity in LPS-stimulated mouse peritoneal macrophages and RAW 264.7 cells. *Biochem. Biophys. Res. Commun. 314*, 695−703.

(36) Bicker, K. L., Subramanian, V., Chumanevich, A. A., Hofseth, L. J., and Thompson, P. R. (2012) Seeing citrulline: Development of a phenylglyoxal-based probe to visualize protein citrullination. *J. Am. Chem. Soc. 134*, 17015−17018.